Astron. Astrophys. 314, 672–678 (1996)

ASTRONOMY AND ASTROPHYSICS

VLBI differential astrometry at large angular separation: 3C 395 – 3C 382

L. Lara[1,2], J.M. Marcaide[3], A. Alberdi[2,4], and J.C. Guirado[5]

[1] Istituto di Radioastronomia, CNR, Via Gobetti 101, I-40129 Bologna, Italy
[2] Instituto de Astrofísica de Andalucía, CSIC, Apartado 3004, E-18080 Granada, Spain
[3] Dpto. de Astronomía y Astrofísica, Universitat de València, E-46100 Burjassot, Valencia, Spain
[4] LAEFF, P.O. Box 50727, E-28080 Madrid, Spain
[5] Jet Propulsion Laboratory, 4800 Oak Grove Dr., Pasadena, CA 91109, USA

Received 14 September 1995 / Accepted 17 March 1996

Abstract. We have observed the pair of radio sources 3C 395 and 3C 382 using Very Long Baseline Interferometry in November 1990, simultaneously at 8.4 and 2.3 GHz. Through the use of differential astrometry techniques we have determined with submilliarcsecond precision the angular separation between these two sources. We have demonstrated the feasibility of differential astrometry for pairs of radio sources separated 6° on the sky, being the reference source a low luminosity radio galaxy. Successive differential astrometry observations would allow to clarify unambiguously the internal kinematics of the quasar 3C 395.

Key words: astrometry - techniques: interferometric – quasars: individual (3C 395) – galaxies: individual (3C 382)

1. Introduction

Very Long Baseline Interferometry (VLBI) provides not just high angular resolution for imaging purposes, but also precise determinations of the positions of radio sources on the sky. The astrometric capabilities of VLBI have produced important results in astronomy. For example, VLBI finds strict limits on the proper motion of quasars, whose stationary character is a basic requirement in standard cosmological models (e.g. Bartel et al. 1986; Marcaide et al. 1994). Regarding extragalactic radio jets, it also makes possible to measure absolute internal proper motions of compact components (e.g. Guirado et al. 1995b), or to study the dependence of the core position with the frequency of observation (Marcaide & Shapiro, 1984). In addition, the direct observation of an apparent core jitter would allow to study with unprecedented detail the physical conditions close to the central engine of active galactic nuclei (Marcaide et al. 1994). The importance of high precision astrometry is also evidenced by the necessity of a quasi-inertial reference frame for astrophysical purposes and spacecraft navigation, which is defined from a network of compact extragalactic radio sources with precise positions accurately determined with VLBI (e.g. Russell et al. 1993).

With the application of VLBI differential astrometry (e.g. Shapiro et al. 1979) it is possible to determine the relative position of a target source with respect to another reference source with precisions as high as tens of microarcseconds. The strategy followed during the observations is to sample the interferometer phases of both radio sources, simultaneously in very close pairs of sources, or, what is more usual, alternately if the angular separation between the two sources is larger than the single antenna beam widths. Then the different contributions to the phase can be removed, to isolate the geometrical contribution which will be finally modelled by adjusting some geometrical parameters with a weighted-least-squares algorithm. The advantage of working with the difference of the phases of both sources lies in the partial or total cancellation of unmodelled contributions coming mainly from the propagation medium and/or instrumentation, while it still contains the precise information about the relative position of the sources. However, the difficulty of the analysis increases with the angular separation between the radio sources: first, the longer the antenna slew time to switch from one source to another, the more difficult the so-called "connection" of the phases from observation to observation; second, at large angular separations, azimuth and elevation dependent contributions to the phase must be accurately described since they never cancel completely; and third, contributions from the propagation medium might not be correlated at large angular separations and thus, the expected cancellation could be minimal. While the first and the second problems could be sorted out with faster antennas and the use of more accurate astrometric models, respectively, the third one poses real limits to the applicability of this astrometric technique.

Up to now, the extreme applications of VLBI phase differential astrometry regard pairs of radio sources with angular separations up to 5° and high flux densities (Elósegui et al. 1993; Guirado et al. 1995a). We present here a new step for-

Send offprint requests to: L. Lara

ward, demonstrating the feasibility of phase-delay differential astrometry on a pair of radio sources, the quasar 3C 395 and the core of the radio galaxy 3C 382, separated by 6° on the sky, with the additional difficulty derived from the low flux density level of the reference radio source, the core of 3C 382 ($S_{8.4GHz}$ ~190 mJy).

2. The radio source 3C 395

3C 395 (1901+319) is identified with a 17th magnitude quasar with a redshift z=0.635 (Hewitt & Burbidge 1987; Gelderman & Whittle 1994). At radio wavelengths, it presents a core-jet structure which, at milliarcsecond scales, consists essentially of two components, A and B, in a position angle of 118° separated by a distance of ~15 milliarcseconds (mas) and stationary with respect to each other. A third weaker component, C, is located between them (see Fig. 1a). VLBI observations before 1990 showed this latter component moving superluminally from component A towards component B with an apparent velocity of ~13 c (Waak et al. 1985), although a strong deceleration was later reported by Simon et al. (1988). Subsequent VLBI observations made in 1990, 1991 and 1992 did not show any evidence of motions in 3C 395 (Lara et al. 1994, 1996).

A possible and perhaps simplistic explanation for this change in the kinematical behaviour of component C would be a direct deceleration of a fast moving superluminal component. However, such deceleration could not be due to changes in the geometry of the path followed by component C, since the flux density of this component did not show the significant variations implied by related changes of the Doppler boosting factor. Other explanations could be invoked, such as a possible undersampling in the monitoring of the compact structure of 3C 395, as possible displacements of the position of the peak of brightness of component A, or as even an apparent deceleration of component C due to phase effects caused by Kelvin-Helmholtz instabilities (see Hardee 1990).

VLBI images obtained by means of hybrid mapping techniques do not allow us to distinguish among the above mentioned possibilities, since those images provide information only about the relative positions of the components of the radio structure with respect to an internal point, which could also be affected by the same kinematics. It is necessary to determine the positions of the components with respect to an external reference point, i.e. a different and unrelated radio source. We took as reference the core of 3C 382 (1833+326), a broad line FR-II radio galaxy with a redshift z=0.0578, at an angular separation of ~6° from 3C 395. At milliarcsecond scales, 3C 382 shows a radio structure strongly dominated by a compact component identified with the core of the radio source (see Fig. 1b; Giovannini et al. 1994). In this paper we report the first application of VLBI differential astrometry on the pair 3C 395/3C 382. A continued application of this technique to this pair should be a most suitable tool to understand the kinematics of 3C 395 since such study would show the internal absolute proper motion of each component in the compact structure.

3. VLBI observations and data analysis

On November 1st 1990 we observed the pair of radio sources 3C 382 and 3C 395 at 2.3 and 8.4 GHz simultaneously, using the Mark III recording system in mode A (Rogers et al. 1983). We observed alternately 3C 395 and 3C 382 with an overall duty cycle of 9 minutes: 2 minutes tracking 3C 395, 4 or 5 minutes tracking 3C 382, and gaps of one minute to allow the antennas to switch from one source to the other (see Lara et al. 1994 for a more detailed description of the observations). The uncertain coordinates available for 3C 382 at the time of the observations forced us to include several blocks of strong and compact calibrators during the experiment in order to guarantee a successful fringe search. This produced undesirable gaps in the sampling of the interferometer observables of the target and reference source, which, together with the non-detection of 3C 382 in several baselines due to the limited integration time required in phase reference observations, forced us to reject several hours of data and a major part of the observing array for the astrometric analysis. We kept a subarray of four antennas which observed 3C 395 and 3C 382 alternately without interruption during 5 hours: Effelsberg (100m, Germany), Onsala (20m, Sweden), Medicina (32m, Italy) and Haystack (37m, USA), still sufficient to provide a precise relative position between the two sources.

During the data analysis, we worked with the interferometer phase delay, τ_ϕ, which in our experiment showed a statistical error 100-to-500-fold smaller than that of the group delay, τ_G, commonly used in the analysis of geodetic experiments. However, the phase delay has the drawback of its related 2π-ambiguity inherent to the interferometer phase, ϕ, from which it is defined. The phase-delay ambiguity is ~120 ps at 8.4 GHz, and ~440 ps at 2.3 GHz. In order to remove the ambiguities from the observed phase delay we followed a similar procedure to that described by Guirado et al. (1995a, and references therein). We used a largely improved version of the astrometry software VLBI3 (Robertson et al. 1975) which estimates, by means of a weighted-least-squares algorithm, the unknown model parameters which are later used to construct theoretical estimates of the interferometer observables.

In Table 1 we present the main fixed model parameters needed for the theoretical models used by VLBI3. The coordinates used for the telescopes, the values of UT1-UTC and the Earth pole coordinates are those given by the Goddard Space Flight Center (GSFC) VLBI Global Solution GLB831, once interpolated to the experiment day. Since GLB831 did not provide the coordinates of 3C 395 or 3C 382, we took the coordinates of 3C 395 (J2000) from the U.S. Naval Observatory (USNO) source position list N9413, referred to epoch 1991.93, and transformed them to the GSFC reference frame using the rotation matrix given by the International Earth Rotation Service (1991 IERS Annual Report). This rotation resulted in a change of 2.6 and 0.1 mas in the right ascension and declination of 3C 395, respectively. We considered the coordinates of 3C 382 as free parameters in our calculations.

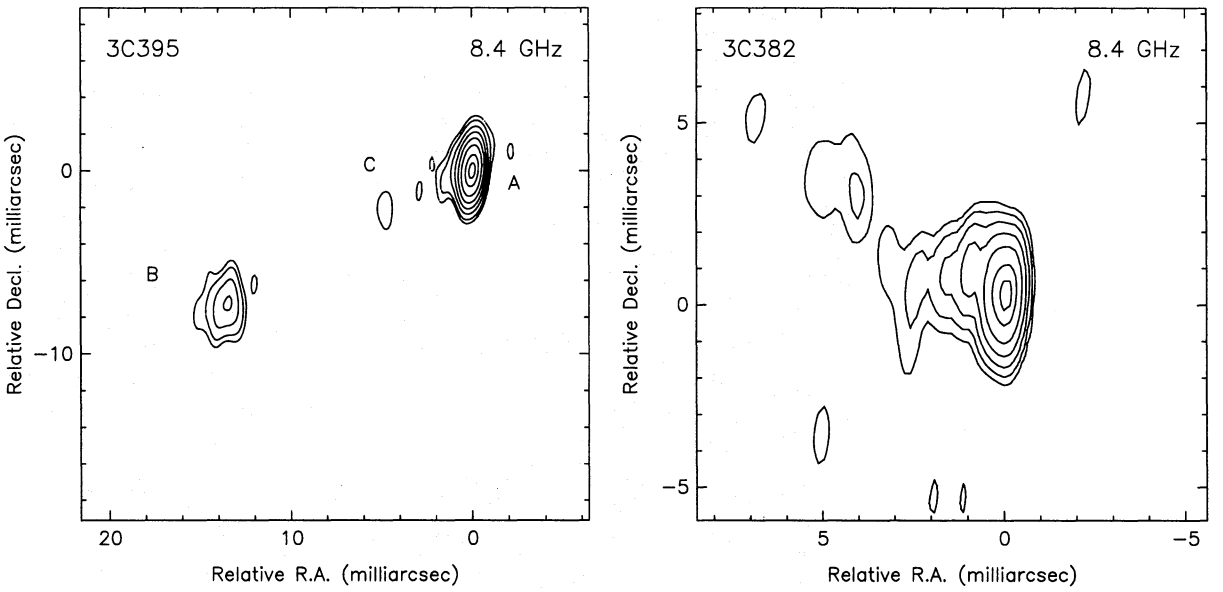

Fig. 1a and b. VLBI maps of 3C 395 **a** and 3C 382 **b** from epoch 1990.84 at 8.4 GHz. The map of 3C 395 is restored with a beam of 2.1×0.6 mas with the major axis along P.A. -2.2° . The contours represent -1,1,2,4,8,16,32, and 64% of the peak brightness of 860 mJy/beam. The map of 3C 382 is restored with a beam of 2×0.5 mas with the major axis along P.A. -6° . The contours represent -2,2,4,8,16,32,64, and 90% of the peak brightness of 74 mJy/beam

Table 1. Fixed input parameters of the theoretical model

J2000.0 source coordinates[1]

3C 395 $\alpha = 19^h\ 02^m\ 55^s.93912$ $\delta = 31°\ 59'\ 41''.7014$

Antenna site coordinates[2]

Antennas	Cylindric coordinates			Axis offsets[3]
	R(m)	Φ(°)	Z(m)	(m)
Effelsberg	4063236.774	-6.8836077	4900430.718	0.0
Haystack	4700478.414	71.4881596	4296881.683	0.0
Medicina	4555159.902	-11.6469302	4449559.089	1.83
Onsala	3444969.142	-11.9263514	5349830.643	0.0

Precession Constant (J2000.0)[4]
P=5028″.989/tropical century

Nutation
Predictions of IAU 1980 Nutation Series

UT1 and Earth Pole Coordinates
GLB831 solutions from GSFC

Earth Tides
Radial Love number, h=0.60967
Horizontal Love number, l=0.085
Tidal lag angle, θ=0.0

Tropospheric zenith delays

τ_{atm}(Haystack)	7.78 ns
τ_{atm}(Effelsberg)	7.62 ns
τ_{atm}(Medicina)	8.15 ns
τ_{atm}(Onsala)	7.80 ns

[1] Taken from the USNO N9411 solutions corresponding to epoch 1991.93, and transformed to the GSFC reference frame (see text)
[2] GLB831 solutions from GSFC, interpolated to the date of the experiment (1990.84)
[3] All the antennas are altitude-azimuth.
[4] From Lieske et al. (1977).

3.1. The connection of the phase delay

The output data after correlation and fringe fitting consisted, for each scan, of the interferometer phase, group delay and phase-delay rate, with their associated errors. We used the group delay and phase-delay rate to calibrate our theoretical astrometric model (in essence, to estimate the clock behaviour for each station). With this model we were able to predict, for each baseline, the number of ambiguities between successive observations of the same source, and hence, generate connected phase delays, τ_ϕ^{con}. The frequency and the observing duty cycle (Δt) determine the accuracy which must be achieved in the phase-delay rate model to insure the phase connection:

$$\dot{\tau}_\phi^{res} \times \Delta t \leq \frac{1}{2\,\nu_r},$$

where $\dot{\tau}_\phi^{res}$ is the residual of the phase-delay rate, i.e. the difference between the observed and the modelled phase-delay rates, and ν_r = 8404.99 MHz is our reference frequency. Given our 9 minute observing duty cycle and our reference frequency, we required to model the phase-delay rate with an accuracy of ± 0.1 ps/s. In Fig. 2 we display the residuals of the phase-delay rate for 3C 395 and 3C 382 after the weighted least-squares fit. Several phase-delay rate data points, mainly corresponding to the noisy baselines Haystack-Onsala and Haystack-Medicina, had to be discarded in the fit but in general, the scatter of the residuals of the phase-delay rate of one radio source is about 0.1 ps/s.

Even so, some ambiguities may remain in τ_ϕ^{con}, which can be detected and eliminated through visual inspection of the phase-delay residuals after a preliminary least-squares analysis using this observable. Additionally, phase closures provide an useful tool to guess the existence of ambiguities and check the goodness of the phase connection, since phase closures must only depart from zero by a small amount due to the source structures (baseline-dependent contributions) if the phase connection is done correctly.

Once the phase is connected for each baseline and each radio source separately, the possible existence of the so-called global ambiguities, i.e. a constant integer number of extra cycles between the phase of one source and the phase of the other, for each baseline has to be considered. We determine these global ambiguities by setting them as free parameters in a preliminary least-squares fit. In our case, the best results were obtained when we added 7 phase ambiguities (7 × 120 ps) to the phase delays of 3C 382 associated to the antenna in Haystack.

3.2. Contribution from the troposphere

The contribution from the neutral atmosphere to the phase delay, τ_{atm}, is dominated by the troposphere, which extends from the ground up to ~11 km. We consider the troposphere as a refractive propagation medium which produces an excess path length, and estimate this excess along the zenith direction assuming an isothermal atmosphere in hydrostatic equilibrium (Saastamoinen, 1973). This model assumes that the excess path length along the zenith has a major contribution (~220 cm) from the dry air, only dependent on the atmospheric pressure at the surface, and a minor contribution (~10 cm) from the concentration of water vapour in the troposphere, concentration which is assumed uniform. The values of the tropospheric zenith delays obtained for each antenna using the meteorological data recorded during the observations are displayed in Table 1.

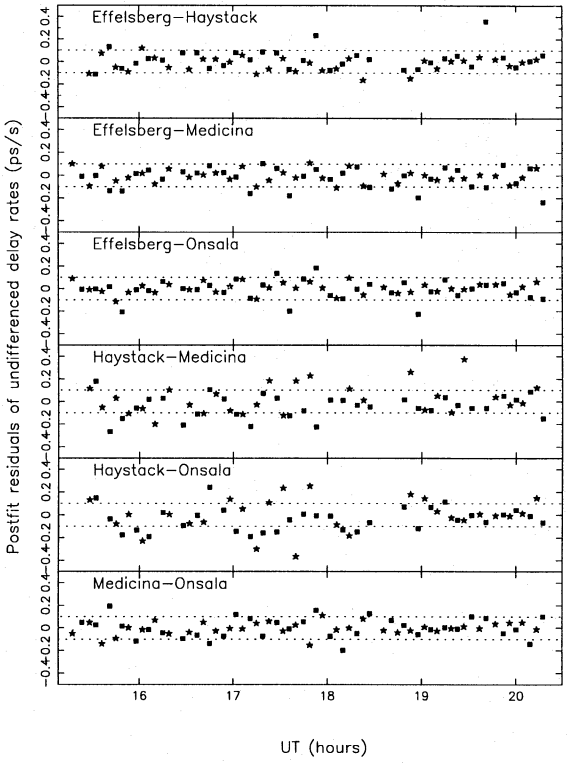

Fig. 2. Postfit residuals of the undifferenced phase-delay rate. The dotted-line represents the accuracy limit of ± 0.1 ps/s. Squares and stars stand for 3C 395 and 3C 382, respectively

For antenna elevations other than the zenith, we used the mapping function derived by Chao (1974), accurate to within 1 cm compared with ray-tracing measurements (Davis et al. 1985) when the antenna elevations are larger than 20° , as was the case for the observations of 3C 382 and 3C 395.

3.3. Contribution from the radio source structure

The contribution from the brightness distribution of a radio source to the phase delay is defined with respect to the position of an arbitrary point, whose criterion and procedure of selection must be well established, mainly if the aim of the observations is to compare results from different epochs. We obtained maps and delta-component models of the milliarcsecond-scale brightness distributions of 3C 395 and 3C 382 after several iterations of hybrid mapping with the Caltech VLBI package (Pearson 1991) (see Fig. 1). For each radio source, we considered as its reference point at 8.4 GHz the position of the peak of brightness of the region identified with the compact core. We then shifted the delta-component models of 3C 395 and 3C 382 so that the reference point was, in both cases, at the origin of coordinates,

and applied the program PHASE of the Caltech VLBI package to determine and subtract the contribution of the structure from the phase delay. This contribution does not exceed the value of 10 ps neither in 3C 395 nor in 3C 382, as expected from their strongly core dominated structures.

Since we used the phase delay at 8.4 and 2.3 GHz to properly remove the ionospheric contribution (see Sect. 3.4), the reference point at 2.3 GHz must be physically identified with that chosen at 8.4 GHz, so opacity effects must be taken into account. To achieve this for 3C 395, we measured, at both frequencies, the position of the peak of brightness of the core with respect to the position of the peak of brightness of component B, which is optically thin at 2.3 and 8.4 GHz (Lara et al. 1994), and thus not affected by opacity effects. Using a super-resolved 2.3 GHz image obtained with half the synthesized beam, we obtained that the peak of the core component at 2.3 GHz was shifted by 0.5 mas along P.A.= 139° with respect to the peak of the core at 8.4 GHz.

3.4. Contribution from the ionosphere

Most of the propagation effects caused by the ionosphere, in particular the contribution to the phase delay τ_{ion}, scale as ν^{-2} due to its dispersive character (Thompson, Moran & Swenson 1986). Our main aim when we observed 3C 395 and 3C 382 at dual frequency, apart from obtaining spectral-index information (Lara et al. 1994), was to make use of this dependence in order to estimate and eliminate the ionospheric plasma contribution to the phase delay. At the time of the observations Effelsberg did not have a 2.3 GHz receiver available, and the remaining array was not sensitive enough to detect clearly the weak core of 3C 382 at this frequency. Thus, we only obtained dual frequency data for the much stronger radio source 3C 395. In order to estimate and remove the ionospheric contribution to the phase delay for 3C 395 and 3C 382, we followed an alternative approximate method, which actually is a mixture of the usual method based on double frequency observations and the method based on the total electron content (TEC) along the line of sight (Klobuchar 1975; see Guirado et al. 1995a for details of the application of this alternative method).

We first followed on the data at 2.3 GHz available for 3C 395 a parallel procedure to that described in Sections 3.1-3 in order to construct a connected and structure-free phase delay at this frequency. Considering the phase delay of 3C 395 at both frequencies and using the ν^{-2} dependence, we estimated the contribution of the ionosphere to its phase delays. In order to estimate the ionospheric contribution for 3C 382 we followed several steps: first, we estimated the TEC model parameters, i.e. the zenith TEC values for each station, by means of a least-squares algorithm which used the dual frequency results obtained on 3C 395; second, once known these parameters, we applied the TEC model to the source 3C 382 to obtain the ionospheric contribution to its phase delays; and third, to estimate the ionospheric contribution in those baselines involving Effelsberg, we assumed that the TEC values obtained for Medicina were also valid for Effelsberg, which is ~1000 km north from

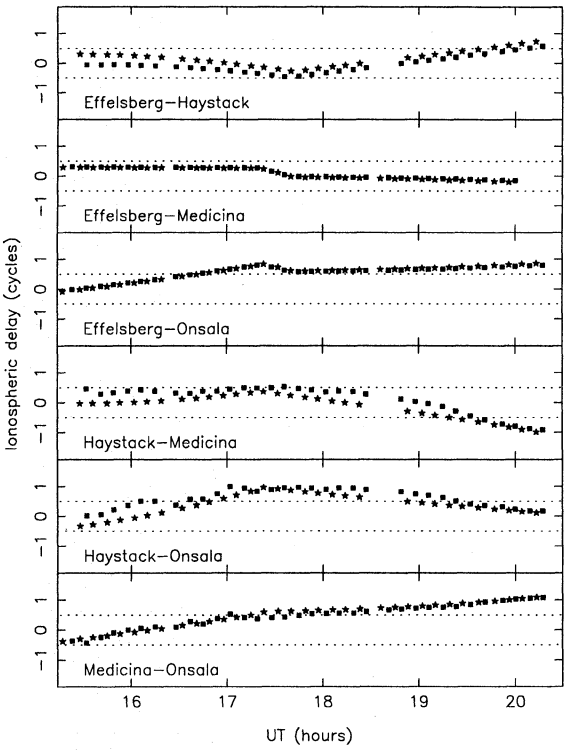

Fig. 3. Ionospheric contribution to the phase delay in the line of sight of 3C 395 (squares) and 3C 382 (stars). For the baselines Haystack-Medicina, Haystack-Onsala and Medicina-Onsala, the contribution for 3C 395 is derived from dual-frequency data. For the baselines with Effelsberg, and for 3C 382 we have used the method described in the text. The dotted-line represents the size of one 2π-phase-related ambiguity

Medicina. The simple procedure described in these steps transforms the ionospheric delay measured in the direction of 3C 395 into that which would be measured in the direction of 3C 382, taking into account the different elevation and azimuth of the antennas between the two directions. In Fig. 3 we display the ionospheric contribution to the phase delays for 3C 395 (derived from double frequency observations except in those baselines with Effelsberg) and 3C 382 (derived from the TEC model), which were later subtracted from the previously connected and structure-free phase delay.

3.5. The differential phase delay

Once the phase delays for both sources were connected and free from structure and ionospheric contributions, we constructed the differential phase delays, τ_ϕ^{diff}, defined as the difference of the phase delays of 3C 382 and the phase delays of 3C 395 in adjacent observing times. For radio sources with a small angular separation, such difference produces the cancellation of effects which cannot be accurately described by the theoretical models. The most efficient situation for differential astrometry results when both radio sources lie inside the beam of each antenna (e.g. 1038+528 A,B: Marcaide & Shapiro 1983) However,

at larger angular separations the cancellations are less efficient and special care must be taken to account for the different times of observations of each radio source, and the azimuth and elevation dependent contributions to the phase delay. Accurate models for these contributions are needed. To achieve such models and also to account for the clock behavior at each antenna, the use of the differential phase delay alone is insufficient, and the phase delay of one of the sources must also be simultaneously used in the least-squares fit. Consequently, we have considered both, the differential phase delay and the phase delay corresponding to 3C 395, as inputs for our final least-squares fit. The weights given to each data set were scaled so that the post-fit root weighted mean square (rms) was unity. Once a good model was obtained, i.e. with residuals well inside one ambiguity range, we interpolated the phase-delay residuals of 3C 395 to the times of observation of 3C 382, and added these interpolated residuals to the theoretical estimates for the phase delay of 3C 395 at those times. With the so-constructed interpolated phase delay of 3C 395 and the observed phase delay of 3C 382 we formed the differential phase delay. With these data we refined our final model and obtained improvements in the unweighted rms of the differential phase-delay residuals ranging from ~50% in the baselines with Effelsberg, to only ~5% in the more noisy baselines Haystack-Medicina and Haystack-Onsala.

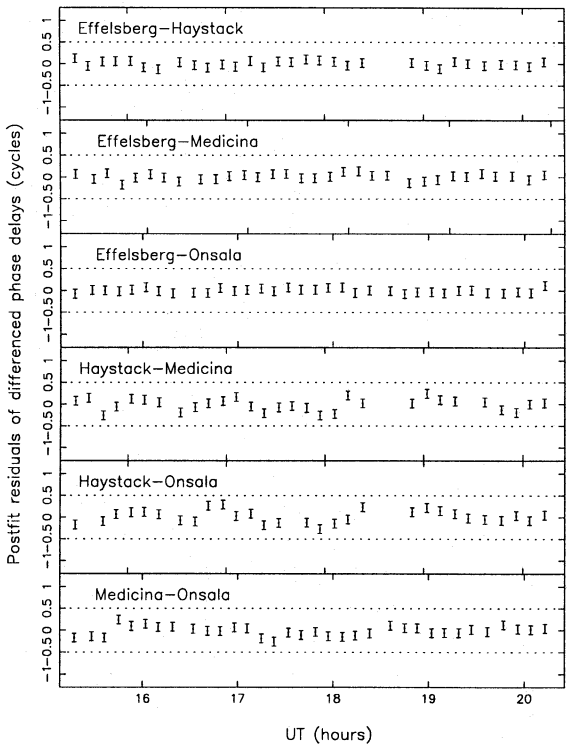

Fig. 4. Postfit residuals of the interpolated differential phase delay after the final least-squares fit. The error bars shown are the standard deviations, which were scaled so that the weighted rms of the postfit residuals was unity. The dotted-line represents the size of one 2π-phase-related ambiguity

4. Results and conclusions

In the final least-squares fit we estimated, without any *a priori* constraint, the right ascension and declination of 3C 382 and the coefficients of a third order polynomial to describe the behaviour of the clock at every antenna but Haystack, set as the reference site. Also included in the least-squares fit, but with their adjustments constrained through a covariance matrix by their *a priori* values (as given in Table 1) and their standard deviations (as given below in parenthesis), were the tropospheric zenith delays (0.2 ns), the site coordinates (2 cm), the coordinates of the Earth's pole (1 mas), UT1-UTC (0.04 ms), and the coordinates of 3C 395 (0.02 ms in R.A. and 0.4 mas in Dec.). To obtain the standard deviation of the coordinates of 3C 395 we added in quadrature the error given by USNO and the estimated error associated with the rotation from the USNO to the GSFC reference frame, and increased the result twofold to be conservative. The rest of standard deviations were taken from Guirado et al. (1995a).

We show in Fig. 4 the residuals for the differential phase delay for the final least-squares fit using the differential phase delay and the phase delay corresponding to 3C 395 as input data. There is still some evidence of systematic effects not accounted for, mainly in those baselines involving Haystack, but in every case the residual trends remain within a half-ambiguity interval during the whole observing time. In Table 2 we show the relative separation between 3C 382 and 3C 395, with their statistical standard errors. We have estimated the error associated with the identification of the peak of brightness in the radio source structure of 3C 395 and 3C 382 (Thompson, Moran & Swenson 1986), and have found that it is negligible (~0.010 mas for each source and coordinate) compared with the statistical standard errors given in Table 2. Similarly, Guirado et al. (1995a) find, after a detailed analysis on a pair of radio sources separated by 5° , that the final error is mainly dominated by the statistical standard errors.

Table 2. Final estimates of the angular separation of 3C 395 and 3C 382

$\Delta\alpha$(3C 395-3C 382)	$27^m\ 52^s.54921 \pm 0^s.00001$
$\Delta\delta$(3C 395-3C 382)	$-42'\ 5''.15376 \pm 0''.00035$

Successive epochs of phase reference observations of 3C 395 and 3C 382 would allow us to know which component, if any, of the radio structure of 3C 395 is moving and, hence, try to clarify the internal kinematics and understand the physical processes in the radio jet of this quasar. Additionally, we have demonstrated the feasibility of the phase connection and the use of VLBI differential astrometry techniques for a pair of radio sources with an angular separation of 6° , being the reference a low power radio source. This result opens the possibility of applying differential astrometry to a much wider sample of radio sources, since within a 6° radius it is possible to find suitable, although in most cases weak, references for almost any radio source. It also brings encouragement to present attempts

to apply this technique to pairs of radio sources at even larger angular separations.

Acknowledgements. We wish to thank the European and the US VLBI networks, the staff of the different observatories for their contribution to the observations, and the MPIfR staff at the correlator for their efforts during the correlation. L.L. acknowledges support from a postdoctoral CSIC grant. J.C.G. holds a National Research Council-NASA Resident Research Associateship award at the JPL, Caltech, under contract with the National Aeronautics and Space Administration. This work has been partially supported by the Spanish DGICYT grant PB89-0009.

References

Bartel N., Herring T.A., Ratner M.I., Shapiro I.I., Corey B.E., 1986, Nature 319, 733
Chao C.C., 1974, JPL/NASA Tech. Rep. N.32-1587, 61
Davis J.L., Herring T.A., Shapiro I.I., Rogers A.E.E., Elgered G., 1985, Radio Science 20, 1593
Elósegui P., Marcaide J.M., Alberdi A., et al., 1993, In: Davis R.J., Booth R.S. (eds.) Sub-arcsecond Radio Astronomy, Cambridge University Press, p.412
Gelderman R., Whittle M., 1994, ApJS 91, 491
Giovannini G., Feretti L., Venturi T., et al., 1994, ApJ 435, 116
Guirado J.C., Marcaide J.M., Elósegui P., et al., 1995a, A&A 293, 613
Guirado J.C., Marcaide J.M., Alberdi A., et al., 1995b, AJ 110, 2586
Hardee P.E., 1990, In: Zensus J.A., Pearson T.J. (eds.) Parsec-Scale Radio Jets, Cambridge University Press, p.266
Hewitt A., Burbidge G., 1987, ApJS 63, 1
International Earth Rotation Service (IERS), Annual Report for 1991, Observatoire de Paris, 1992
Klobuchar J.A., 1975, Air Force Cambridge Research Laboratories, Report No. AFCRL-TR-75-0502, (NTIS ADA 018862)
Lara L., Alberdi A., Marcaide J.M., Muxlow T.W.B., 1994, A&A 285, 393
Lara L., Muxlow T.W.B., Alberdi A., et al., 1996, submitted to A&A.
Lieske J.H., Lederle T., Fricke W., 1977, A&A 58, 1
Marcaide J.M., Shapiro I.I., 1983, AJ 88, 1133
Marcaide J.M., Shapiro I.I., 1984, ApJ 276, 56
Marcaide J.M., Elósegui P., Shapiro I.I., 1994, AJ 108, 368
Robertson D.S., 1975, Ph.D. thesis, Massachusetts Institute of Technology
Rogers A.E.E., Capallo R.J., Hinteregger H.F., et al., 1983, Science 219, 51
Russell J.L., Fey A.L., Jauncey D.L., et al., 1993, In: Davis R.J., Booth R.S. (eds.), Sub-arcsecond Radio Astronomy, Cambridge University Press, p.397
Saastamoinen J., 1973, Bull. Géodésique 105, 279
Shapiro I.I., Wittels J.J., Counselman III C.C., et al., 1979, AJ 84, 1459
Simon R.S., Johnston K.J., Spencer J.H., 1988, In: Reid M.J., Moran J.M. (eds.) Proc. IAU Symp. 129, The Impact of VLBI on Astrophysics and Geophysics, Kluwer Academic Publishers, p.21
Thompson A.R., Moran J.M., Swenson G.W., 1986, Interferometry and Synthesis in Radio Astronomy, Wiley (New York)
Waak J.A., Spencer J.H., Johnston K.J., Simon R.S., 1985, AJ 90, 1989

This article was processed by the author using Springer-Verlag LaTeX A&A style file version 3.